Defect creation in amorphous-silicon thin-film transistors

C. F. O. Graeff, M. S. Brandt, and M. Stutzmann
Walter Schottky Institut, Technische Universität München, Am Coulombwall, 85478 Garching, Germany
M. J. Powell
Philips Research Laboratories, Redhill, Surrey RH1 5HA, United Kingdom
(Received 24 March 1995)

We report on the threshold voltage shift and its origin in amorphous-silicon thin-film transistors with a nitride gate insulator. These transistors were subjected to two different degradation methods: (i) applying a strong gate bias at 450 K for a prolonged period of time (thermal bias annealing), and (ii) pulse light soaking at room temperature. To characterize metastable defects in these transistors, we propose and demonstrate the usefulness of spin-dependent photoconductivity (SDPC). For the light-soaked samples both a threshold voltage shift and an increase in defect density are observed, in contrast to the thermal-bias-annealing (TBA) treatments where threshold voltage shifts are observed, but no change in the defect density is detected with SDPC. The results are consistent with the main effect of TBA being the creation of states in the lower part of the band gap.

Instability effects in hydrogenated amorphous silicon (*a*-Si:H) and related devices have attracted considerable attention because of their negative consequences for device performance. Of particular interest are instabilities of *a*-Si:H-based thin-film transistor (TFT's). TFT's are susceptible to photodegradation, but more important are threshold voltage shifts observed under prolonged bias stress (the application of a gate voltage for long periods). The origin of the threshold voltage shift after bias stress is still controversial. There are two possible explanations: The first describes the voltage shift by charge trapping in slow states located in the amorphous-silicon nitride (*a*-SiN:H) dielectric,[1–7] the second by metastable creation of additional defect states in the amorphous silicon at the interface.[1–4,6,8–10] However, so far no direct microscopic evidence for or against either mechanism has been reported in the literature. Commonly, electron-spin resonance (ESR) is one of the most powerful technique to identify and study defects in semiconductors. Unfortunately, due to the small dimensions of conventional TFT's and the low defect density of the *a*-Si:H layer necessary for making useful devices, conventional ESR lacks sufficient sensitivity to provide any information about such devices. In contrast to conventional ESR, spin-dependent photoconductivity (SDPC) detects paramagnetic states not by directly monitoring the resonant microwave absorption due to spin-flip transitions but by recording changes of the conductivity as a result of selection rules for recombination.[11–19] SDPC is more sensitive to paramagnetic states by orders of magnitude compared to conventional ESR (for example by a factor of 10^5 in the case of our TFT's) and is also applicable under standard operation conditions of devices. In particular, SDPC has been applied with success to elucidate several processes involved in recombination in *a*-Si:H,[11–15] *a*-Si_xGe_{1-x}:H,[19] *p-i-n* and *n-i-n* devices of *a*-Si:H,[17,18] as well as in crystalline Si devices.[16] In the present work, the SDPC technique is applied to *a*-Si:H TFT's in different degradation states with the aim to improve our understanding of instabilities in these devices.

The amorphous-silicon thin-film transistors studied here are state of the art inverted-staggered TFT's, with silicon nitride as the gate insulator.[20] The *a*-Si:H layer is about 300 nm thick, while the nitride is 400 nm thick. The TFT's used could be illuminated both from the gate and source/drain electrodes. The gate electrode was a semitransparent Cr layer (about 30 nm), and the source and drain contacts consisted of interdigit electrodes with a width to length ratio (W/L) varying from 230 to 994 ($L=50\ \mu$m). For the SDPC experiments, the TFT's were illuminated with a tungsten lamp (approximately 60 mW/cm^2) using an RG650 cutoff filter, and kept at a constant temperature (100 K $< T <$ 300 K). The samples were placed in the TE_{102} cavity of a standard *X*-band ESR spectrometer. The spin-dependent change of the photoconductivity was measured by modulating the static magnetic field (H_0) and using lock-in detection of the photocurrent. The source drain voltage (V_{sd}) was kept low (1 V $< V_{sd} <$ 3 V) to keep the field distribution as homogeneous as possible along the channel.

In order to study the instability mechanism in the TFT's, two different degradation methods were employed: (i) bias-temperature stressing (or thermal bias annealing, TBA) with bias voltages V_{ba} between -20 and 20 V applied for 30 min at a temperature of $T_{ba}=450$ K, and (ii) pulsed light soaking (or light-induced degradation, LID) using a xenon flash lamp with a pulse width of $\approx 2\ \mu$s and a pulse repetition rate of 300 Hz, leading to an average illumination intensity of 100 mW cm^{-2}.[21] For the second degradation method, TFT's were illuminated at room temperature for different periods of time, with strongly absorbed light from the gate side, to make sure that the defects were mostly generated at the interface *a*-Si:H/*a*-SiN:H.

Figure 1 shows examples of transfer characteristics after different degradation treatments. The normalized transfer characteristics are shown as sheet conductance G $(\Omega/\square)^{-1}$ against the induced surface charge Q (electrons/cm^2).[20] The use of G and Q removes dependences on geometrical parameters of the TFT. The arrows indicate the respective threshold voltage (V_{th}) as defined in Ref. 20. In Fig. 1(a) it is clearly seen that the effect of thermal bias annealing under a positive bias is much more pronounced than under a negative bias. This

0163-1829/95/52(7)/4680(4)/$06.00

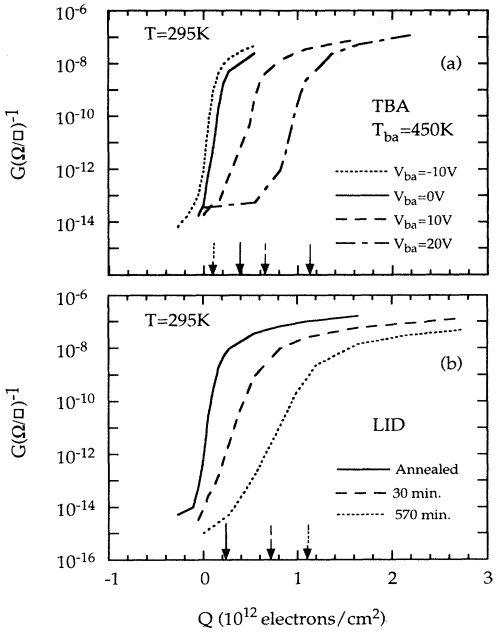

FIG. 1. Sheet conductance $G(\Omega/\Box)^{-1}$ against induced surface charge Q (electrons/cm^2) measured at room temperature after different degradation treatments. (a) After thermal bias annealing the TFT at 450 K for 30 min under different gate bias V_{ba}. (b) After light-induced creation of defects at room temperature, for different soaking times. The arrows indicate the induced surface charge corresponding to the respective threshold voltage.

is most probably due to the n^+ contact design of the TFT's, allowing electron but no hole injection. The TBA treatments had little or no effect on the electron-field-effect mobility (μ_{fe}), which for our samples is between 0.6 and 0.7 cm^2 V^{-1}s^{-1} in the annealed state. Although a pronounced V_{th} shift is observed after TBA treatments, there is only a small decrease (a factor of 1.6) in the subthreshold slope even for TBA with $V_{ba}=20$ V. If the density of states between the Fermi level and the tail states were constant, then the prethreshold slope in the logarithmic transfer characteristics would be roughly inversely proportional to the square root of the density of states ($N(E)$).[8,20] From this result alone one can expect a rather small increase in $N(E)$ above midgap. In Fig. 1(b) the effects of light-induced creation of defects are presented. In the LID case not just V_{th} changed, but the subthreshold slope changed quite dramatically (by a factor of 11.7 after 570-min illumination), indicating a corresponding strong increase in $N(E)$ above midgap. We also observed a decrease in μ_{fe} after illumination (from 0.7 to 0.2 cm^2 V^{-1}s^{-1} after the 570-min light soaking), a possible explanation comes from the light-induced degradation of the source drain contacts. Note that the overall V_{th} shifts in Fig. 1 are similar for both TBA and LID treatments.

Typical SDPC results are presented in Fig. 2. The experiments are made by recording the photocurrent changes when the sample is brought into spin resonance. One should observe a decrease of the photocurrent in resonance, but due to the detection scheme (modulation of

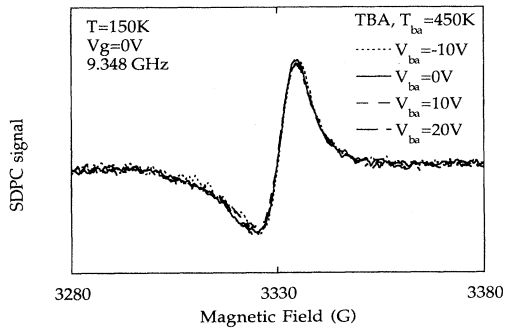

FIG. 2. Typical SDPC spectra taken at 150 K with a source-drain voltage of 1 V and zero gate voltage. The different curves correspond to different degradation states of the TFT (thermal bias annealing at 450 K for 30 min under different gate bias).

the magnetic field and lock-in detection) the first derivative of the SDPC signal is seen in Fig. 2. From spin angular momentum conservation, if the final state after recombination is a spin singlet state ($S=0$), the initial configuration in the case of nonradiative recombination must also be a singlet state. A microwave field, strong enough to saturate the ESR of either the electron or hole, will produce an isotropic spin distribution in which the probabilities of singlet and triplet configurations will be $\frac{1}{4}$ and $\frac{3}{4}$, respectively. This will produce a change in recombination rate if the initial distribution was not isotropic, or in other words if there was initially an excess of triplet or singlet states. Such a deviation from isotropy can basically be of two types, using the nomenclature of Movaghar, Ries, and Schweitzer:[22] (i) normally spin dependent (NSD) or (ii) anomalously spin dependent (ASD). In the NSD case, the spin polarization due to the external magnetic field (H_0) creates an excess of triplet states. In the ASD case, prior to recombination the electron and hole are spatially correlated and form a pair. Knowing that the singlets have a shorter recombination lifetime (τ) than triplet states, their steady-state concentration will be smaller than in the isotropic situation. As discussed elsewhere,[19] the two models predict differences in the SDPC signal intensity ($\Delta\sigma/\sigma$) and its dependence on temperature, defect density, etc. As an example, and of special interest here, for the NSD case $\Delta\sigma/\sigma$ is small (of the order of 3×10^{-6} at room temperature) and basically independent of defect density, whereas for the ASD case $\Delta\sigma/\sigma$ can be as high as 10^{-1}, and under certain conditions linearly dependent on the defect density.[14] What distinguishes the two extremes is the relation between the spin-lattice-relaxation time T_1 and the recombination lifetime τ.[19] In the ASD case, T_1 for both spins involved in the recombination must be greater than τ. Then the spin state of the pair is long lived and the recombination of an individual pair is subjected to the full spin selection rule ($\Delta S=0$). If this condition is not fulfilled, the spins flip many times before recombination takes place, and thus the difference between singlet and triple pairs is lost.

As discussed elsewhere,[12,15] the a-Si:H signal at 150 K is composed of two contributions. The first comes from the nonradiative recombination of an electron in the

conduction-band-tail state captured by a neutral deep defect (or dangling bond) state, with $g=2.0050$ and linewidth $\Delta H_{pp}=9$ G. The second contribution is due to holes hopping in the valence-band tail, with $g=2.01$ and $\Delta H_{pp}=20$ G. This explains the observed asymmetric line shape shown in Fig. 2. No significant changes in the line shape are observed after the degradation treatments, as can be seen in this figure.

The sensitivity of $\Delta\sigma/\sigma$ to changes in the defect density (N_{db}) was found to be strongly temperature dependent. The signal at 150 K or below is proportional to the defect density, whereas at room temperature the dependence on the defect density is small. This result is in agreement with previous SDPC studies on *a*-Si:H thin films. At room temperature only a slight increase of $\Delta\sigma/\sigma$ (a factor of 10) with the increase in defect density (by a factor of 200) has been observed.[11] At lower temperatures (150 K), in comparison, $\Delta\sigma/\sigma$ is essentially found to be a linear function of defect density.[13] We propose the following explanation for the temperature dependence of $\Delta\sigma/\sigma$ versus N_{db}, leaving a more detailed discussion to a forthcoming publication. In Fig. 3 we plot T_1 for electrons occupying the conduction-band tail (cb), holes in the valence-band tail (vb), and dangling-bond (db) states as a function of temperature.[23] In the same picture an estimate of τ for two different defect densities is also presented by the shaded areas. To estimate τ we have used the product $\mu\tau N_{db}=2.5\times10^{8}$ $(\mathrm{V\,cm})^{-1}$ (mobility, recombination lifetime, and defect density) obtained by Street, Zesch, and Thompson,[24] which is basically temperature independent. Two values for N_{db} were chosen, corresponding roughly to the expected values at the annealed and degraded states. μ was chosen to be between 0.1 and 1 $\mathrm{cm^2\,V^{-1}s^{-1}}$ at room temperature, decreasing by a factor of 100 at 100 K. Note that the values of μ conflict in the literature, especially in what concerns its temperature dependence. As can be seen from Fig. 3, only at 150 K and below is T_1 comparable to τ; thus anomalous SDPC and consequently a strong dependence of $\Delta\sigma/\sigma$ on N_{db} is expected. Note that the values for T_1 (cb) were obtained in heavily doped samples, which thus have a high electron concentration in the conduction band. As discussed in Ref. 23, thermal excitation and/or interaction with thermally excited carriers lead to a rapid reduction in relaxation times. Since at zero or slightly negative gate voltages, the number of thermally excited carriers in the conduction band is smaller by orders of magnitude than in heavily doped *a*-Si:H samples, the plotted value for T_1 (cb) is surely a lower limit, and can be in reality one order of magnitude higher.

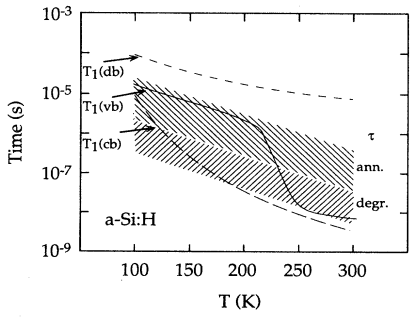

FIG. 3. Spin-lattice-relaxation time (T_1) and recombination lifetime (τ) as functions of temperature. The curves correspond to the spin-relaxation times in *a*-Si:H for dangling bonds (db), conduction-band-tail states (cb), and valence-band-tail states (vb) after Ref. 23. The shaded areas correspond to the estimated recombination lifetimes for an annealed *a*-Si:H sample ($N_{db}\approx10^{16}$ $\mathrm{cm^{-3}}$) and a degraded sample ($N_{db}\approx10^{17}$ $\mathrm{cm^{-3}}$).

In Fig. 4, $\Delta\sigma/\sigma$ is plotted against $Q-Q_{th}$ where Q_{th} is the surface-induced charge at threshold voltage. As can be seen, there is no significant change in $\Delta\sigma/\sigma$ after TBA treatments. In fact the use of $Q-Q_{th}$ instead of Q corrects for the threshold voltage shift, and all curves fall on top of each other. Note that the gate voltage (or Q) dependence of the SDPC signal reflects the changes of the relative densities of the various charge states of the dangling bond with a shift of Fermi energy (E_F). Since our TFT's are unipolar, out study is restricted to the upper part of the density of states, although a limited movement of E_F toward the valence band is expected due to the photogeneration of holes. Positive gate bias moves E_F toward the conduction band, charging part of the neutral dangling bonds (D_0) negatively. Since SDPC is only sensible to D_0 state, the transition $D_0\rightarrow D_-$ for positive Q is reflected by a decrease in $\Delta\sigma/\sigma$. This also happens in some cases for high negative bias (although not shown) due to the positive charging of part of the D_0. (Further work on ambipolar or *p*-type TFT's is necessary to clarify this point.)

In contrast, as can be seen in Fig. 5, the LID treatment induces a clear increase in $\Delta\sigma/\sigma$ for all gate voltages. In Fig. 5 for clarity we present only the extreme cases (annealed and fully degraded). In Table I we compare our SDPC-deduced N_{db} changes using $\Delta\sigma/\sigma\propto N_{db}$, with the expected N_{db} changes from Ref. 21, as well as the calculated defect density using the prethreshold slope in the logarithmic transfer characteristics.[8,20] Good agreement is found.

These results are in agreement with those in Ref. 1–7 and 9, which also observed no or small changes in defect density in the upper part of the *a*-Si:H band gap, but a

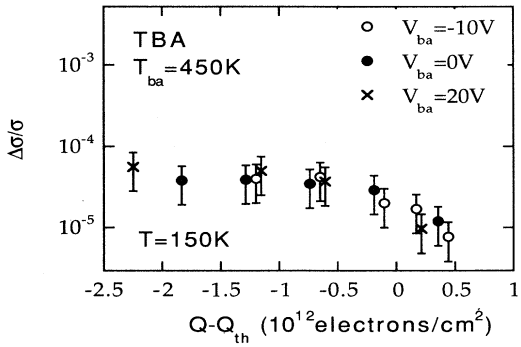

FIG. 4. SDPC signal amplitude ($\Delta\sigma/\sigma$) measured at 150 K vs $Q-Q_{th}$. The different symbols correspond to different thermal bias annealing treatments.

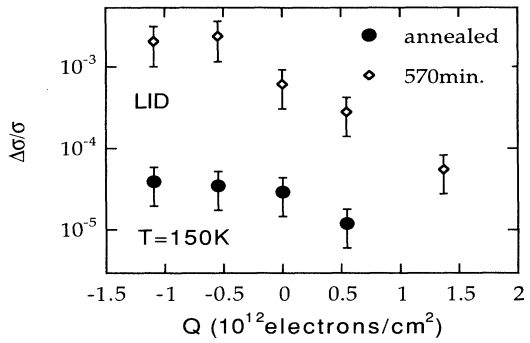

FIG. 5. SDPC signal amplitude ($\Delta\sigma/\sigma$) measured at 150 K vs the induced surface charge Q, for a TFT in the annealed state (open diamond), and the light-soaked state (closed circle).

strong shift in the *I-U* characteristic after similar TBA treatments in *a*-Si:H TFT's with a nitride insulator. The results are consistent with the main effect of TBA being the creation of states in the lower part of the band gap,[8] even though charging of the nitride cannot be ruled out.

Further work on ambipolar TFT's, where E_F can be moved both into the upper and lower parts of the band gap, would be helpful to clarify the effects of TBA on the defect density of states. Also of interest would be the use of TFT's with an oxide insulator, where the effects of TBA on the density of dangling bonds are predicted to be more pronounced (in Ref. 10 N_{db} changes by approximately a factor of 100 after positive TBA treatments are reported).

In summary, we have demonstrated the applicability of spin-dependent photoconductivity (SDPC) as a powerful quantitative tool to study defect states in *a*-Si:H-based thin-film transistors. It is shown that at low temperatures (150 K) and zero or small negative bias, the SDPC signal is proportional to the density of neutral dangling bond states in or close to the channel. The technique was applied to TFT's after thermal-bias-annealing (TBA) and light-induced-degradation (LID) treatments. Both degradation methods were found to be effective in changing the *I-U* (or *G-Q*) characteristic of the studied TFT, but only the LID degradation was found to produce an increase in the *a*-Si:H layer defect density above midgap. Our results are consistent with the main effect of TBA being the creation of states in the lower part of the band gap.

TABLE I. Light-induced defect creation using pulsed light illumination, as a function of time. The ESR data were taken from Ref. 21, while the *I-U* data points were calculated from the subthreshold slope changes of the *I-U* (or *G-Q*) characteristics (Refs. 8 and 20). The SDPC defect density changes were deduced for a signal amplitude proportional to N_{db}.

LID soaking time (min)	$N_{db}(t)/N_{db}(0)$		
	ESR	*I-U*	SDPC
0	1	1	1
30	10±5	5±2	7±2
570	20±5	12±5	20±5

C.F.O.G. acknowledges support from the Alexander von Humbolt Stiftung (Germany).

[1]W. B. Jackson and M. D. Moyer, Phys. Rev. B **36**, 6217 (1987).
[2]M. J. Powell, C. van Berkel, I. D. French, and D. H. Nicholls, Appl. Phys. Lett. **51**, 1242 (1987).
[3]N. Nickel, W. Fuhs, and H. Mell, J. Non-Cryst. Solids **115**, 159 (1989).
[4]N. Nickel, W. Fuhs, and H. Mell, Philos. Mag. B **61**, 251 (1990).
[5]A. V. Gelatos and J. Kanicki, Appl. Phys. Lett. **57**, 1197 (1990).
[6]J. Kanicki, C. Godet, and A. V. Gelatos, in *Amorphous Silicon Technology—1991,* edited by A. Madan, Y. Hamkawa, M. Thompson, P. C. Taylor, and P. G. LeComber, MRS Symposia Proceedings No. 219 (Materials Research Society, Pittsburgh, 1991), p. 45.
[7]J. P. Kleider, C. Longeaud, D. Mencaraglia, A. Rolland, P. Vitrou, and J. Richard, J. Non-Cryst. Solids **164-166**, 739 (1993).
[8]S. C. Deane, F. J. Clough, W. I. Milne, and M. J. Powell, J. Appl. Phys. **73**, 2895 (1993).
[9]P. N. Morgan, W. I. Milne, S. C. Deane, and M. J. Powell, J. Non-Cryst. Solids **164-166**, 199 (1993).
[10]S. C. Deane and M. J. Powell, J. Appl. Phys. **74**, 6655 (1993).
[11]R. A. Street, Philos. Mag. B **46**, 273 (1982).
[12]H. Dersch, L. Schweizer, and J. Stuke, Phys. Rev. B **28**, 4678 (1983).
[13]K. Lips and W. Fuhs, J. Non-Cryst. Solids **137&138**, 255 (1991).
[14]M. S. Brandt and M. Stutzmann, in *Amorphous Silicon Materials and Solar Cells,* edited by B. L. Stafford, AIP Conf. Proc. No. 234 (AIP, New York, 1991).
[15]K. Lips, S. Schütte, and W. Fuhs, Philos. Mag. B **65**, 945 (1992).
[16]A recent review is given by C. H. Seager, E. L. Venturini, and W. K. Schubert, J. Appl. Phys. **71**, 5059 (1992).
[17]K. Lips and W. Fuhs, J. Appl. Phys. **74**, 3993 (1993).
[18]M. S. Brandt, M. Stutzmann, and J. Kocka, J. Non-Cryst. Solids **164-166**, 693 (1993).
[19]C. F. O. Graeff, M. Stutzmann, and M. S. Brandt, Phys. Rev. B **49**, 11 028 (1994).
[20]M. J. Powell, IEEE Trans. Electron Devices **36**, 2753 (1989).
[21]M. Stutzmann, M. C. Rossi, and M. S. Brandt, Phys. Rev. B **50**, 11 592 (1994).
[22]B. Movaghar, B. Ries, and L. Schweitzer, Philos. Mag. B **41**, 159 (1980).
[23]M. Stutzmann and D. K. Biegelsen, Phys. Rev. B **28**, 6256 (1983).
[24]R. A. Street, J. Zesch, and M. J. Thompson, Appl. Phys. Lett. **43**, 672 (1983).